Molecular Pharmacology Fast Forward. Published on November 19, 2014 as DOI: 10.1124/mol.114.095471
This article has not been copyedited and formatted. The final version may differ from this version.

(4-(Bis(4-fluorophenyl)methyl)piperazin-1-yl)(cyclohexyl)methanone hydrochloride (LDK1229): A New Cannabinoid CB1 Receptor Inverse Agonist from the class of benzhydryl piperazine analogs

Mariam M. Mahmoud, Teresa Olszewska, Hui Liu, Derek M. Shore, Dow P. Hurst, Patricia H. Reggio, Dai Lu and Debra A. Kendall

Department of Molecular and Cell Biology, University of Connecticut, Storrs, Connecticut, 06269, United States (M.M.M.); Irma Lerma Rangel College of Pharmacy, Texas A&M Health Science Center, Kingsville, Texas, 78363, United States (T.O., H. L., D.L.); Department of Chemistry and Biochemistry, University of North Carolina at Greensboro, Greensboro, NC 27402, United States (D.M.S., D.P.H., P.H.R.); Department of Pharmaceutical Sciences, University of Connecticut, Storrs, Connecticut, 06269, United States (D.A.K.)

Molecular Pharmacology Fast Forward. Published on November 19, 2014 as DOI: 10.1124/mol.114.095471
This article has not been copyedited and formatted. The final version may differ from this version.

Running title:
CB1 inverse agonist LDK1229

Corresponding Author:
Debra A. Kendall
69 N. Eagleville Rd, Department of Pharmaceutical Sciences, University of Connecticut
Storrs, CT 06269
Email: debra.kendall@uconn.edu.

Number of:
Text pages 44
Tables 4
Figures 5
References 59

Number of words:
Abstract 249
Introduction 728
Discussion 939

Non-Standard Abbreviations:
[^{35}S]GTPγS: guanosine 5′-*O*-(3-[^{35}S]thio)triphosphate; 5HT-2α: serotonin receptor type 2α; BSA: Bovine serum albumin; CB_1: cannabinoid receptor type 1; CB_2: cannabinoid receptor type 2; CP55,940: 5-(1,1-dimethylheptyl)-2-(5-hydroxy-2-(3-hydroxypropyl)cyclohexyl)phenol; GFP: green fluorescent protein; GPCR: G-protein-coupled receptor; HEK293: Human Embryonic Kidney 293 cells; MAPK: mitogen-activated protein kinase; PBS: Phosphate-buffered saline; SR141716A: rimonabant; SR144528: N-((1S)-endo-1,3,3-trimethyl bicyclo heptan-2-yl)-5-(4-chloro-3-methylphenyl)-1-(4-methylbenzyl)-pyrazole-3-carboxamide); TME: Tris-Mg^{2+}- EDTA; TMH: transmembrane helix; WIN55,212-2: (R)-(+)-[2,3-dihydro-5-methyl-3-(4-morpholinylmethyl) pyrrolo-[1,2,3-d,e]-1,4-benzoxazin-6-yl]-1-naphthalenyl-methanone.

Molecular Pharmacology Fast Forward. Published on November 19, 2014 as DOI: 10.1124/mol.114.095471
This article has not been copyedited and formatted. The final version may differ from this version.

ABSTRACT

Some inverse agonists of the cannabinoid CB_1 receptor have been demonstrated to be anorectic antiobesity drug candidates. However, the first generation of CB_1 inverse agonists, represented by rimonabant (SR141716A), otenabant and taranabant, are centrally active with a high level of psychiatric side effects. Hence, the discovery of CB_1 inverse agonists with a chemical scaffold distinct from these holds promise for developing peripherally active CB_1 inverse agonists with fewer side effects. We generated a new CB_1 inverse agonist (4-(Bis(4-fluorophenyl)methyl)piperazin-1-yl)(cyclohexyl)methanone hydrochloride (LDK1229) from the class of benzhydryl piperazine analogs. This compound binds to CB_1, more selectively than CB_2, with a K_i value of 220 nM. Comparable CB_1 binding was also observed by analogs 1-(Bis(4-fluorophenyl)methyl)-4-cinnamylpiperazine dihydrochloride (LDK1203) and 1-(Bis(4-fluorophenyl)methyl)-4-tosylpiperazine hydrochloride (LDK1222) which differed by the substitution on the piperazine ring where the piperazine of LDK1203 and LDK1222 are substituted by an alkyl group and by a tosyl group, respectively. LDK1229 exhibits efficacy comparable to SR141716A in antagonizing the basal G protein coupling activity of CB_1 as indicated by a reduction in GTPγS binding. Consistent with inverse agonist behavior, increased cell surface localization of CB_1 upon treatment with LDK1229 was also observed. Although docking and mutational analysis showed that LDK1229 forms similar interactions with the receptor as SR141716A, the benzhydryl piperazine scaffold is structurally distinct from the first generation CB_1 inverse agonists; it offers new opportunities for developing novel CB_1 inverse agonists through optimization of molecular properties such as the polar surface area and hydrophilicity, to reduce the central activity observed with SR141716A.

Molecular Pharmacology Fast Forward. Published on November 19, 2014 as DOI: 10.1124/mol.114.095471
This article has not been copyedited and formatted. The final version may differ from this version.

INTRODUCTION

The cannabinoid receptors are members of the class A superfamily of G protein coupled receptors (GPCRs). The cannabinoid receptor 1 (CB_1) is present in high abundance throughout the central nervous system (Howlett, 1995) but is also expressed in a number of peripheral tissues, such as the cardiovascular and reproductive systems as well as the gastrointestinal tract (Batkai et al., 2001; Croci et al., 1998; Engeli et al., 2005), and is involved in substance addiction, chronic pain, memory and metabolic and inflammatory disorders (Howlett et al., 2004; Mackie, 2006; Pertwee, 2006). A second subtype of the cannabinoid receptors, the cannabinoid receptor 2 (CB_2), is predominantly found in immune cells and non-neuronal tissues (Galiegue et al., 1995) and is implicated in a variety of modulatory functions, including immune suppression, induction of apoptosis, and induction of cell migration (Basu and Dittel, 2011).

The CB_1 receptor preferentially couples to the $G_{i/o}$ type of G proteins (Howlett and Fleming, 1984) and has been functionally linked to the inhibition of adenylate cyclase (Slipetz et al., 1995) and the activation of mitogen-activated protein kinases (MAPKs), including extracellular signal-regulated kinase-1 and -2, p38 MAPK, and c-Jun *N*-terminal kinase (Ahn et al., 2012; Bouaboula et al., 1996; Turu and Hunyady, 2010). In addition, it is associated with the inhibition of N- and P/Q-type voltage-dependent Ca^{2+} channels and the stimulation of A-type and inwardly rectifying K^+ channels (Howlett, 2005).

As is common for many GPCRs (De Lean et al., 1980), the CB_1 receptor may exist in multiple activation states that are promoted by its binding to different ligands. Upon binding to receptor agonists, such as the endogenous arachidonylethanolamide and 2-arachidonyl glycerol, or the synthetic agonists CP55,940 and WIN55,212-2, the active form of the receptor predominates. Interestingly, the CB_1 receptor possesses agonist-independent constitutive or basal

Molecular Pharmacology Fast Forward. Published on November 19, 2014 as DOI: 10.1124/mol.114.095471
This article has not been copyedited and formatted. The final version may differ from this version.

activity which can be inhibited by inverse agonists (Pertwee, 2005). This ligand-independent activity led to a receptor model that accounts for multiple activation states (Gether and Kobilka, 1998; Ghanouni et al., 2001) with distinct biochemical characteristics, including extent and selectivity of G protein or β-arrestin coupling (Kenakin, 1995).

Inverse agonists of the CB_1 receptor have attracted considerable attention in drug discovery because of their ability to regulate appetite and manage substance addiction (Janero, 2012; Janero and Makriyannis, 2009; Silvestri and Di Marzo, 2012). Consequently, considerable effort has been invested in discovering compounds that can regulate the constitutive activity of the CB_1 receptor. However, SR141716A (rimonabant) (Rinaldi-Carmona et al., 1994), the only CB_1 inverse agonist to be briefly clinically marketed in Europe for the control of obesity (Moreira and Crippa, 2009), was removed from use due to its severe neuropsychiatric side effects including mood-depressant actions (Despres et al., 2005; Traynor, 2007). The first generation of CB_1 inverse agonists are commonly derived from diaryl analogs of pyrazole (e.g. SR141716A) or pyrazole bioisosteres such as imidazole, triazole, thiazole and pyrazoline (Lange and Kruse, 2005; Lange and Kruse, 2008; Muccioli and Lambert, 2005). However, most of these are brain penetrant due to their physicochemical nature (Chorvat, 2013) and will likely generate unwanted side effects in the central nervous system. In an effort to develop new CB1 inverse agonist scaffolds, we analyzed the common pharmacophore of this class of compounds that was proposed by Lange et al (Lange and Kruse, 2005). This showed that the biaryl groups connecting to a central heteroaromatic ring are pivotal in forming aromatic stacking interactions with CB1 receptors (McAllister et al., 2004; Shim et al., 2012). This brought our attention to the benzhydryl piperazine scaffold, which exhibits a similar structure to the common pharmacophore of CB1 inverse agonists in lieu of the biaryl heteroaromatic ring moiety. Hence, we synthesized a

Molecular Pharmacology Fast Forward. Published on November 19, 2014 as DOI: 10.1124/mol.114.095471
This article has not been copyedited and formatted. The final version may differ from this version.

group of benzhydryl piperazine analogs, and demonstrated that some of the synthesized analogs, LDK1203, LDK1222 and LDK1229, exhibited inverse agonist binding profiles for the CB1 receptor. In addition to its binding profile to the CB_1 receptor, LDK1229's inverse agonism is evident from its effect on basal as well as agonist-induced G protein coupling, and its impact on the internalization and cell surface expression of CB_1. Docking studies using a model of the inactive CB_1 receptor showed that LDK1229 forms interactions with the receptor consistent with inverse agonist SR141716A. Discovering new and improved means for inhibiting the activity of CB_1 is critical for understanding the constitutive activity of CB_1 and for developing new therapeutic agents for treating substance addiction and disorders associated with CB_1 activity.

Molecular Pharmacology Fast Forward. Published on November 19, 2014 as DOI: 10.1124/mol.114.095471
This article has not been copyedited and formatted. The final version may differ from this version.

MATERIALS AND METHODS

Synthesis. The benzhydrylpiperazine analogs LDK1203, LDK1222 and LDK1229 were synthesized by alkylation, tosylation and acylation of the 1-(4,4′-difluorobenzhydryl)piperazine (Figure 1A). The employed 1-(4,4′-difluorobenzhydryl)piperazine (III) was prepared by monoalkylation of piperazine with 4,4′-difluorobenzhydryl chloride (II) that was obtained by halogenation of 4,4′-difluorobenzhydryl methanol (I) with oxalyl chloride as previously reported (Weïwer et al., 2012). The obtained free bases of the benzhydrylpiperazine analogs were then converted to their corresponding hydrochloric salts by reacting with an ethereal solution of HCl. The chemical identity of the newly synthesized compounds is as follows: LDK1203 is 1-(Bis(4-fluorophenyl)methyl)-4-cinnamylpiperazine dihydrochloride, LDK1222 is 1-(Bis(4-fluorophenyl)methyl)-4-tosylpiperazine hydrochloride and LDK1229 is (4-(Bis(4-fluorophenyl)methyl)piperazin-1-yl)(cyclohexyl)methanone hydrochloride. The structure confirmation data for the free bases of LDK1203, LDK1222 and LDK1229 are as follows. LDK1203: ^{1}H NMR (500 MHz, Chloroform-*d*) δ 7.28-7.40 (m, 8H), 7.23 (t, *J* = 7.5 Hz, 1H), 6.99 (t, *J* = 7.5 Hz, 4H), 6.53 (d, *J* = 15 Hz, 1H), 6.28 (d, *J* = 15 Hz, 1H), 4.26 (s, 1H), 3.22 (d, *J* = 6 Hz, 2H), 2.24-2.78 (m, 8H). MS (EI): *m/z* = 404.21 (M^{+}). LDK1222: ^{1}H NMR (500 MHz, Chloroform-*d*) 7.64 (d, *J* = 7.9 Hz, 2H), 7.36 (d, *J* = 7.9 Hz, 2H), 7.22-7.31 (m, 4H), 6.94 (t, *J* = 8.4 Hz, 4H), 4.22 (s, 1H), 2.91-3.10 (m, 4H), 2.48 (s, 3H), 2.38-2.47 (m, 4H). MS (EI): *m/z* = 442.15 (M^{+}). LDK1229: ^{1}H NMR (500 MHz, Chloroform-*d*) δ 7.35 (dd, *J* = 8.2, 5.5 Hz, 4H), 6.99 (t, *J* = 8.2 Hz, 4H), 4.22 (s, 1H), 3.61 (t, *J* = 5 Hz, 2H), 3.42 (t, *J* = 5 Hz, 2H), 2.43 (t, *J* = 5 Hz, 2H), 2.42 (t, *J* = 5 Hz, 2H), 2.31-2.40 (m, 4H), 1.74-1.82 (m, 2H), 1.65-1.73 (m, 3H), 1.44-1.56 (m, 2H). MS (EI): *m/z* = 398.2 (M^{+}).

Molecular Pharmacology Fast Forward. Published on November 19, 2014 as DOI: 10.1124/mol.114.095471
This article has not been copyedited and formatted. The final version may differ from this version.

Plasmid Construction. All mutants were generated by site-directed mutagenesis (QuickChange; Stratagene, La Jolla, CA) using the human CB1 cDNA cloned into pcDNA3.1 as a template, according to the manufacturer's instructions. All mutations were confirmed by DNA sequencing.

CB_1 Expression and Membrane Preparation. Human embryonic kidney 293 (HEK293) cells were maintained in Dulbecco's modified Eagle's medium supplemented with 10% fetal bovine serum and 3.5 mg/ml glucose at 37°C in 5% CO_2. For transient expression of the receptors, HEK293 cells were seeded at 800,000 cells/100-mm dish on the day prior to transfection and transfected with 5-10 μg of the wild type or mutant human CB1 receptor cloned into pcDNA3.1 using the calcium phosphate precipitation method (Chen and Okayama, 1987). At 24 h post-transfection, membranes of transfected cells expressing either the wild-type or mutant receptors were prepared as described previously (Ahn et al., 2009).

Radioligand Binding Assay. In the homologous and heterologous competition binding experiments, approximately 7.5 μg of wild-type CB_1, CB_2 or mutant CB_1 membrane was incubated at 30°C for 60 min with a fixed tracer ([^{3}H]CP55,940, 141.2 Ci/mmol, [^{3}H]SR141716A, 56 Ci/mmol, or [^{3}H]WIN55,212-2, 52.2 Ci/mmol, PerkinElmer Life Sciences (Boston, MA)) concentration typically at its K_d, which was determined from saturation binding isotherms (see results for details). Binding assays were performed with at least nine concentrations of unlabeled competitor ligand (ranging between 100 *p*M and 100 μM) as described previously (Ahn et al., 2012). Nonspecific binding was determined in the presence of 1 μM unlabeled CP55,940, SR141716A or WIN55,212-2. Reactions were terminated by adding 300 μL of TME buffer containing 5% BSA followed by filtration with a Brandel cell harvester through Whatman GF/C filter paper. Radioactivity was measured by liquid scintillation counting.

Molecular Pharmacology Fast Forward. Published on November 19, 2014 as DOI: 10.1124/mol.114.095471
This article has not been copyedited and formatted. The final version may differ from this version.

The total assay volume and the amount of membrane samples were adjusted to avoid ligand depletion by keeping the bound ligand less than 10% of the total.

GTPγS Binding Assay. GTPγS binding assays were performed as described previously (Ahn et al., 2012). Briefly, 7.5 μg of membranes were incubated for 60 min at 30°C in a total volume of 200 μL GTPγS binding assay buffer (50 mM Tris-HCl, pH 7.4, 3 mM $MgCl_2$, 0.2 mM EGTA, and 100 mM NaCl) with unlabeled test compounds as indicated, 0.1 nM [^{35}S]GTPγS (1250 Ci/mmol; PerkinElmer Life Sciences, Boston, MA), 3 μM GDP (Sigma, St. Louis, MO), and 0.1% (w/v) BSA. 3 μM GDP was used to increase the window of basal activity. Nonspecific binding was determined with 10 μM unlabeled GTPγS (Sigma, St. Louis, MO). The reaction was terminated by rapid filtration through Whatman GF/C filters. The radioactivity trapped in the filters was determined by liquid scintillation counting.

Confocal Microscopy and Image Quantification. HEK293 cells were transfected with the CB_1 receptor carboxyl terminally fused to GFP using Lipofectamine (Invitrogen) according to the manufacturer's instructions. The CB1-GFP expressing cells were seeded onto 35-mm glass-bottomed dishes (Matek, MA) pre-coated with poly-D-lysine. Cells were treated with different compounds for various lengths of time and then washed twice with PBS, followed by fixation with 4% paraformaldehyde for 10 min at room temperature. Images were acquired using a Leica confocal laser scanning microscope and detection of GFP was carried out following excitation at 488 nm. Quantification of the fluorescence intensity was achieved by using the Quantitative Imaging of Membrane Proteins (QuimP) software (http://go.warwick.ac.uk/bretschneider/quimp) (Bosgraaf et al., 2009; Dormann et al., 2002), a set of plug-ins for the open source program ImageJ (http://rsb.info.nih.gov/ij/). The Boa plug-in was used to detect the cell surface and checked against the cell edge in the transmitted image of

Molecular Pharmacology Fast Forward. Published on November 19, 2014 as DOI: 10.1124/mol.114.095471
This article has not been copyedited and formatted. The final version may differ from this version.

each cell. The Ana plugin was then used to read the cell contours produced by the Boa plugin and compute the ratio of fluorescence intensity on the cell surface to the average intensity of the cell interior fluorescence. The results are representative of at least four independent transfections and 6 different images for each condition. Untransfected cells exhibited no apparent fluorescence under the experimental conditions that were used. The parameters for all of the acquired images and their consequent analysis were kept constant throughout.

Ligand and GTPγS Binding Data Analysis. All ligand binding assays and GTPγS binding assays were carried out in duplicate. Data are presented as the mean ± S.E. value or the mean with the corresponding 95% confidence limits from at least three independent experiments. K_i values were calculated using the Cheng-Prusoff equation (Cheng and Prusoff, 1973) based on K_d values obtained from saturation binding analyses. The binding constants for the wild-type and mutant receptors were compared using analysis of variance (ANOVA) followed by Bonferroni's post hoc test for significance. *p* values of <0.05 were considered to be statistically significant.

Computational Methods

Conformational Analysis of LDK1229. To generate a library of low-energy conformers of LDK1229, the Spartan Conformation Distribution protocol was used (Wavefunction, Inc., Irvine, CA). In this protocol, the algorithm systematically searches through all rotatable bonds and ring conformations (*e.g.* alternate chair conformations for flexible rings). The energy of each conformer generated was calculated using the Merck Molecular Force Field (MMFF94S). This calculation yielded 68 unique conformations of LDK1229. The geometry and energy of these 68 conformations was refined by performing *ab initio* HF-6-31G* energy minimizations on each conformer. To calculate the difference in energy between the global minimum energy conformer and its final docked conformation, rotatable bonds in the global minimum energy conformer

Molecular Pharmacology Fast Forward. Published on November 19, 2014 as DOI: 10.1124/mol.114.095471
This article has not been copyedited and formatted. The final version may differ from this version.

were driven to their corresponding value in the final docked conformation and the single-point energy of the resultant structure was calculated at the HF 6-31G* level.

Template Rationale. Our CB_1 inactive state model was initially constructed by using the 2.8 Å x-ray crystal structure of bovine rhodopsin (Rho) as a template (Palczewski et al., 2000). We chose rhodopsin for several reasons: **(1)** Rhodopsin has an intact "ionic lock" ($R3.50^{214}$-E/$D6.30^{338}$), which is the hallmark of the Class A GPCR Inactive state. **(2)** The cannabinoid receptors and rhodopsin have very hydrophobic binding pockets. Crystal structures reveal that the N-terminus of rhodopsin/opsin is closed over the binding pocket, preventing access from the extracellular milieu (Palczewski et al., 2000; Park et al., 2008; Scheerer et al., 2008). It is very likely that CB1, with its 112 residue N-terminus, is also closed off to the extracellular milieu. Instead, rhodopsin/opsin have been reported to have lipid portals that are used for entry and exit via the lipid bilayer for 11-cis-retinal/trans-retinal as they are shuttled into and out of the receptor (Hildebrand et al., 2009). There is evidence from simulations (Hurst et al., 2010) and from experimental covalent labeling studies (Pei et al., 2008; Picone et al., 2005) that the cannabinoid receptors also possess a portal between TMH6 and TMH7 through which ligands enter. **(3)** In addition, the cannabinoid receptors and rhodopsin share an unusual, GWNC motif sequence motif at the extracellular (EC) end of TMH4. Here a Trp forms an aromatic stacking interaction with $Y5.39^{275}$. This interaction influences the EC positions of TMH3-4-5.

CB_1 Inactive State Model. A sequence alignment between the sequence of the human CB_1 receptor (Gerard et al., 1991) and the sequence of bovine rhodopsin was constructed, using highly conserved residues as an alignment guide; in addition, the hydrophobicity profile of the sequence was also considered when constructing the sequence alignment. Residues in the bovine rhodopsin structure were then mutated to those of human CB_1. The Monte Carlo/simulated

Molecular Pharmacology Fast Forward. Published on November 19, 2014 as DOI: 10.1124/mol.114.095471
This article has not been copyedited and formatted. The final version may differ from this version.

annealing technique Conformational Memories was used to sample the conformational space of TMH6 (Barnett-Norris et al., 2002); this is because TMH6 is known to undergo a functionally-necessary conformational change upon G protein-mediated signaling. For the inactive state model, the chosen TMH6 conformer was one that enabled the formation of a salt bridge between the highly conserved TMH6 residue D6.30^{338} and the highly conserved TMH3 residue R3.50^{214}. This salt bridge (also termed the "ionic lock") has been shown to be important in maintaining the inactive state in the β_2 adrenergic (Ballesteros et al., 2001) and 5HT-2α receptors (Visiers et al., 2002). Extracellular and intracellular loops were added to the model using Modeller (Marcu et al., 2013). SR141716A was docked (within the TMH3-4-5-6 region) in this CB_1 inactive state model and the energy of the complex was minimized, as previously described (Hurst et al., 2006).

Glide Docking of LDK1229 at the CB_1 Receptor (Inactive Conformation). The docking program, Glide (version 5.7, Schrödinger, LLC, New York, NY, 2011), was used to explore possible receptor binding modes of LDK1229. First, the SR141716A-CB_1 binding site was chosen as a starting point for Glide docking studies because of the similar pharmacology between SR141716A and LDK1229. Second, LDK1229 displaces SR141617A in competitive binding experiments, suggesting some commonality between their binding sites. Thus, Glide was used to generate a grid centered on the center-of-mass of our previously reported binding site for SR141716A at the CB_1 receptor (Hurst et al., 2002; McAllister et al., 2004; McAllister et al., 2003). The grid dimensions were 26 Å x 26 Å x 26 Å; this grid size allowed Glide to thoroughly explore the receptor for possible binding site(s). In addition, the results of previously reported mutagenesis and synthetic studies suggest that SR141716A forms an important interaction with K3.28^{192} that is necessary for its ability to act as an inverse agonist of G protein-mediated

Molecular Pharmacology Fast Forward. Published on November 19, 2014 as DOI: 10.1124/mol.114.095471
This article has not been copyedited and formatted. The final version may differ from this version.

signaling (Hurst et al., 2006; Hurst et al., 2002). Therefore, Glide was required to dock LDK1229 in such a way so that it formed a hydrogen bond with $K3.28^{192}$. The only other constraint used was the requirement that LDK1229 must be docked within the exploration grid. Standard precision was selected for the docking setup. 68 conformations of LDK1229 were flexibly docked using Glide. ***The best Glide dock was chosen for subsequent calculations.*** The chosen Glide dock was minimized, using the minimization protocol, described below.

Receptor Model Energy Minimization Protocol. The energy of the LDK1229-CB_1 complex, including loop regions, was minimized using the OPLS 2005 force field in Macromodel 9.9 (Schrödinger, LLC, New York, NY, 2011). An 8.0-Å extended nonbonded cutoff (updated every 10 steps), a 20.0-Å electrostatic cutoff, and a 4.0-Å hydrogen bond cutoff were used in the calculation. The minimization was performed in two stages. In the first stage, the TMH backbone was frozen; this constraint was used to preserve secondary structure while allowing the ligand and TMH side chains to relax. In addition, loop residues were frozen, until they could be minimized using an appropriate dielectric (in the next stage of the minimization). No constraints were placed on the ligands during this stage. The minimization consisted of a conjugate gradient minimization using a distance-dependent dielectric of 2.0, performed in 1000-step increments until the bundle reached the 0.05 kJ/mol gradient. In the second stage of the calculation, the helices and ligand were frozen, but the loops were allowed to relax. The generalized Born/surface area continuum solvation model for water as implemented in Macromodel was used. This stage of the calculation consisted of a Polak–Ribier conjugate gradient minimization in 1000-step increments until the bundle reached the 0.05 kJ/mol gradient.

Molecular Pharmacology Fast Forward. Published on November 19, 2014 as DOI: 10.1124/mol.114.095471
This article has not been copyedited and formatted. The final version may differ from this version.

RESULTS

Chemistry. The free base forms of LDK1203, LDK1222 and LDK1229 were synthesized according to the scheme illustrated in Figure 1A, then purified by Combiflash chromatography followed by conversion to hydrochloric salts to increase shelf life and aqueous solubility. Confirmation data for their structure by mass spectroscopy and ^{1}H NMR are presented in Materials and Methods. Representative first generation inverse agonists, Rimonabant, Otenabant, Taranabant and Ibipinabant are shown for comparison (Figure 1B).

LDK1229 and its Analogs Exhibit Inverse Agonist Binding Profiles. To elucidate the nature of these new compounds, we performed ligand binding studies using membrane preparations from HEK293 cells transfected with CB_1. All three compounds competed with CP55,940 and SR141716A, an agonist and inverse agonist of CB_1, respectively. Using [^{3}H]CP55,940 (K_d = 2 nM) as a tracer, LDK1203, LDK1222 and LDK1229 bound wild-type CB1 with K_i values of 260 nM, 331 nM and 220 nM, respectively. Similarly while using [^{3}H]SR141716A as a tracer (K_d = 5 nM), the compounds also bound with comparable affinities (K_i = 297 nM, 366 nM and 246 nM, respectively; Tables 1-3). The structures of LDK1203 and LDK1222 differed from LDK1229 by the substitution groups on the piperazine ring where the piperazine ring of LDK1203 was substituted by an alkyl group and the piperazine of LDK1222 was substituted by a tosyl group.

Since LDK1229 exhibited the strongest binding affinity among the compounds, it was further investigated for its capability to bind CB_1 receptors in the active and inactive states to confirm its nature as a CB_1 inverse agonist. The CB_1 receptor in the active and inactive states can be readily mimicked by our previously engineered mutant CB_1 receptor models (T210I and T210A) (D'Antona et al., 2006). CB_1 with the T210I mutation was shown to adopt a fully active

Molecular Pharmacology Fast Forward. Published on November 19, 2014 as DOI: 10.1124/mol.114.095471
This article has not been copyedited and formatted. The final version may differ from this version.

form in comparison with the CB_1 wild-type. In contrast, CB_1 with the T210A mutation adopts an inactive state. A GPCR in its active state displays enhanced affinity towards agonists but decreased affinity towards inverse agonists, whereas the inactive state of the receptor exhibits the opposite binding properties such that inverse agonists show higher binding affinity than agonists (Cotecchia et al., 1990; D'Antona et al., 2006; McWhinney et al., 2000; Wade et al., 2001). Hence, our mutant CB_1 receptor models provide ideal tools to evaluate the inverse agonism of LDK1229.

As expected for an inverse agonist, using [^{3}H]SR141716A as the tracer, the binding affinity of LDK1229 to the inactive T210A receptor was enhanced (K_i = 68 nM) relative to its affinity to the wild-type CB_1 receptor (K_i = 246 nM; Table 2). A comparable trend is observed with the inverse agonist, SR141716A, that binds T210A with the highest affinity (K_i = 1.47 nM), and progressively weaker affinity for the wild-type CB_1 (K_i = 5.23 nM), and then the T210I receptor (K_i = 14.7 nM). The ratio of binding affinity for the wild-type receptor relative to the mutant receptor for LDK1229 and SR141716A also reflects the preference of these two compounds for the inactive T210A receptor (Table 2).

Using [^{3}H]CP55,940 as the tracer, and examining binding of the agonist CP55,940, the pattern is reversed (Table 3); CP55,940 binds T210A most weakly and then progressively exhibits enhanced affinity for the wild-type CB_1 and the T210I receptors. This is consistent with its agonist properties. In contrast, LDK1229 binds CB_1 wild-type more tightly than the T210I receptor consistent with inverse agonist binding profiles (D'Antona et al., 2006). For the constitutively active T210I receptor, a large decrease in the binding affinity of LDK1229 compared to the binding affinity of the agonist CP55,940 (5831 nM versus 0.835 nM) is observed. The ratio of binding affinity for the wild-type receptor relative to the mutant receptor

Molecular Pharmacology Fast Forward. Published on November 19, 2014 as DOI: 10.1124/mol.114.095471
This article has not been copyedited and formatted. The final version may differ from this version.

for LDK1229 and CP55,940 is also given for comparison (Table 3). At the extremes, when using [^{3}H]CP55,940 as a tracer, we cannot detect any specific binding with T210A, nor when using [^{3}H]SR141716A as a tracer can we detect any specific binding with T210I, up to 32 μM of LDK1229. Taken together these data suggest that LDK1229's increased binding affinity to T210A over wild-type and its decreased binding affinity to T210I result from the compounds' inverse agonist mode of action.

LDK1229 Inhibits Basal and Agonist-induced G Protein Coupling in a Concentration-dependent Manner. Given the inverse agonist properties observed in the binding profile of LDK1229 to the wild-type and mutant CB_1 receptors, [^{35}S]GTPγS binding assays were performed in its presence. This assay monitors the level of G protein activation by determining the extent of binding of the nonhydrolyzable GTP analog to Gα subunits. We investigated the effects of LDK1229 on the basal G protein coupling activity levels of the wild-type CB_1 receptor (Figure 2A). Interestingly, using 1 μM of LDK1229 in the absence of CP55,940 substantially reduced the basal level of [^{35}S]GTPγS binding from 110 fmol/mg to 70 fmol/mg. We also evaluated its impact on agonist CP55,940-induced [^{35}S]GTPγS binding in the presence of various concentrations of LDK1229. We observed a progressive decrease in the specific GTPγS binding with increasing concentration of LDK1229 up to 32 μM for the CB_1 wild-type receptor (Figure 2B).

Like LDK1229, LDK1203 produced an antagonizing effect on the basal and the agonist-induced levels of [^{35}S]GTPγS and is included for comparison (Figure 2). The antagonizing effect is consistent with the properties of an inverse agonist that promotes the inactive form of the receptor and suggests that this compound inhibits G protein coupling.

Molecular Pharmacology Fast Forward. Published on November 19, 2014 as DOI: 10.1124/mol.114.095471
This article has not been copyedited and formatted. The final version may differ from this version.

LDK1229 Promotes Cell Surface Expression of the CB_1 Receptor. Upon prolonged exposure to an agonist, GPCRs become desensitized and subsequently internalize in the cell. Inverse agonists, however, act in the opposite manner by promoting GPCR localization to the cell surface (Marion et al., 2004; Rinaldi-Carmona et al., 1998b). To assess the effect of LDK1229 on CB_1 cellular localization, we determined the cellular response of CB_1 upon LDK1229 treatment using confocal microscopy of cells expressing GFP-tagged CB_1 receptors. Previous observations (Leterrier et al., 2004; Martini et al., 2007; Rozenfeld and Devi, 2008) indicate that CB_1 is partially constitutive and that much of the wild-type CB1 receptor (~85%) is localized on intracellular vesicles. Using the CB1-GFP chimera expressed in HEK293 cells and treated with vehicle alone (0.03% DMSO), we found that about 15% of CB_1 is present at the plasma membrane but that the pattern of receptor fluorescence within the cells was intracellularly punctate, suggesting that a substantial proportion of receptors is internalized consistent with its basal activity (Figure 3). Treatment with 0.1 μM of the agonist CP55,940 resulted in a further shift toward internalization and a punctate appearance of the CB_1-GFP receptor within the cells (data not shown). In contrast, treatment with 1 μM SR141716A or 10 μM LDK1229 resulted in approximately 20% cell surface localization evident within 3 h and an increase to about 65% of cell surface localization after 5 h (Figure 3B). This is strikingly different from the cell surface localization of 13% for basal cells at 5 h. Taken together, these data further support the inverse agonist activity of LDK1229.

LDK1229 Docked in the CB_1 receptor (Inactive) Model. Since LDK1229 exhibited the strongest binding affinity among the compounds, Glide docking studies were performed and suggest that LDK1229 binds in the TMH3-4-5-6 region of CB_1. This is the same region that forms the binding site for SR141716A at CB_1. Figure 4A and 4C illustrate SR141716A (shown

Molecular Pharmacology Fast Forward. Published on November 19, 2014 as DOI: 10.1124/mol.114.095471
This article has not been copyedited and formatted. The final version may differ from this version.

in cyan) docked in the CB_1 inactive state model. The hydrogen bonding interaction is consistent with our prior CB_1 mutant cycle studies which indicated that the amide oxygen of SR141716A interacts directly with K3.28[192]. This interaction is critical for the inverse agonist properties of SR141716A (Hurst et al., 2006; Hurst et al., 2002).

At its binding site, SR141716A also forms several aromatic-stacking interactions. First, the SR141716A dichlorophenyl ring forms aromatic T-stacks with F3.36[200] and W5.43[279] (shown in orange, see Figure 4A). In addition, the SR141716A chlorophenyl ring forms off-set parallel aromatic stacks with Y5.39[275] and W5.43[279] (shown in orange); In addition, SR141716A forms hydrophobic interactions with W6.48[356]. These aromatic interactions are consistent with our prior mutagenesis studies (McAllister et al., 2004; McAllister et al., 2003) which indicated that SR141716A interacts within an aromatic microdomain in CB_1, which comprised of F3.36[200], Y5.39[275], W5.43[279] and W6.48[356]. Finally, SR141716A forms hydrophobic interactions with L3.29[193], V3.32[196], and L6.51[359] (shown in lime, see Figure 4C). In the ligand-free CB_1 receptor, the F3.36[200]/W6.48[356] aromatic stacking interaction is instrumental to the maintenance of the CB_1-inactive state (McAllister et al., 2004). The binding of SR141716A stabilizes the F3.36[200]/W6.48[356] aromatic stacking interaction through the formation of an extensive network of aromatic stacks within the ligand-receptor complex (Shim et al., 2012).

Figures 4B and 4D illustrate the final docked conformation of LDK1229 (shown in lavender) in the CB_1 inactive state model (Data Supplement). Like SR141716A, the LDK1229 amide oxygen forms a hydrogen bond with K3.28[192] (shown in yellow). The geometry of this hydrogen bond is not optimal, however, because the hydrogen bond distance is longer than found for SR141716A (2.8 Å vs. 2.6 Å) and because the hydrogen bond angle deviates more from linearity than that formed with SR141716A (157° vs. 171°). This suggests that the interaction

Molecular Pharmacology Fast Forward. Published on November 19, 2014 as DOI: 10.1124/mol.114.095471
This article has not been copyedited and formatted. The final version may differ from this version.

between LDK1229 and K3.28[192] is weaker than the interaction between SR141716A and K3.28[192]. The importance of this difference between SR141716A and LDK1229 is discussed in more detail below.

Like SR141716A, LDK1229 also docks in the CB_1 TMH3-4-5-6 aromatic microdomain, but the geometry of its interactions differ somewhat from SR141716A. The fluorophenyl ring of LDK1229 forms aromatic T-stacking interactions with W6.48[356] and W5.43[279] (shown in orange, see Figure 3 (B)). In addition, the other fluorophenyl ring of LDK1229 forms off-set parallel aromatic stacking interactions with Y5.39[275] and W5.43[279] (shown in orange). However, LDK1229 does not form an aromatic stacking interaction with F3.36[200]. This is due to a difference in how the two compounds are oriented within the receptor. Finally, LDK1229 also forms several hydrophobic interactions with residues F3.36[200] (shown in orange), L3.29[193], V3.32[196], and L6.51[359] (shown in lime).

Mutational Analysis of Computationally Predicted Residues in the LDK1229 binding pocket. To test the LDK1229 binding-site hypothesis generated by the receptor model, selective mutation of key residues in the CB_1 receptor were generated. The K3.28[192]A, W5.43[279]A, W6.48[356]A, or C7.42[386]M mutant CB_1 receptors were generated. Our results showed that the K3.28[192]A mutant receptor resulted in total ablation of [^{3}H]CP55,940 binding at wild-type CB_1 and that this residue is critical for CP55,940 binding consistent with previous data (Song and Bonner, 1996). Therefore, competition binding assays on the K3.28[192]A mutant were performed using [^{3}H]WIN55,212-2 as a tracer since [^{3}H]WIN55,212-2 binding to the K3.28[192]A mutant was not significantly different than its binding to the wild-type receptor (K_d = 8.6 nM versus K_d = 4.5 nM). Competition binding analysis revealed that the binding of LDK1229 (K_i = 1316 nM) was affected 6-fold by this mutation compared to wild-type (K_i = 324 nM; Table 4)

Molecular Pharmacology Fast Forward. Published on November 19, 2014 as DOI: 10.1124/mol.114.095471
This article has not been copyedited and formatted. The final version may differ from this version.

suggesting that this residue may be important for a hydrogen bonding interaction with LDK1229. These results alone cannot tell us the specific region on LDK1229 with which K3.28^{192} interacts, but modeling studies reported here suggest that K3.28^{192} hydrogen bonds with the carboxyl oxygen of LDK1229. The K3.28^{192}A mutation results reported here are consistent with previous CB1 K3.28^{192}A mutation studies which showed that K3.28^{192}A is an important interaction site (Hurst et al., 2002) for the carboxamide oxygen of SR141716A (Hurst et al., 2006).

Saturation (equilibrium) binding analysis for [^{3}H]CP55,940 at the other three mutant receptors, W5.43^{279}A, W6.48^{356}A, and C7.42^{386}M, showed that the affinity parameters obtained for the mutant receptors were not significantly different from the K_d at the wild-type CB_1 receptor (K_d for mutants = 6 nM, 4 nM, and 3 nM respectively) suggesting these receptors were properly folded. Therefore, competition binding assays on these mutants were performed using [^{3}H]CP55,940 as a tracer. The W5.43^{279}A mutation had the most profound effect on LDK1229 binding compared to any of the other mutations and showed only 39% displacement of [^{3}H]CP55,940 when using 32 μM of LDK1229. This result is consistent with the modeling studies that suggest that W5.43^{279}A is central in the formation of the aromatic T-stacking interactions with the two fluorophenyl rings in LDK1229. The W6.48^{356}A mutant affected LDK1229 binding by 9-fold (K_i = 1987 nM) and the C7.42^{386}M mutant by 5-fold (K_i = 1010 nM; Table 4). The result for the W6.48^{356}A mutation further supports the modeling results which suggest that this mutation participates in direct aromatic stacking interactions with one of the fluorophenyl rings of LDK1229 consistent with prior studies (McAllister et al., 2003). As shown in Table 4, we found here that enlarging the residue at position 7.42 via the C7.42^{386}M mutation results in a 5-fold loss in affinity for LDK1229 consistent with previous studies by Farrens and colleagues (Fay et al., 2005). Taken together, the results of all mutation studies are consistent

Molecular Pharmacology Fast Forward. Published on November 19, 2014 as DOI: 10.1124/mol.114.095471
This article has not been copyedited and formatted. The final version may differ from this version.

with the modeling results reported here, specifically that LDK1229 occupies the same general binding region as SR1417167A.

LDK1229 has Diminished Activity for CB_2. Based on both binding and functional data, LDK1229 showed some selectivity for the CB_1 receptor over the CB_2 receptor (Figure 5). This is evident by LDK1229's 3-fold reduced binding affinity (K_i= 633 nM; Figure 5A) to the CB_2 receptor compared to the CB_1 receptor (K_i= 220 nM; Table 3) using [^{3}H]CP55,940 as a tracer. This selectivity is also evident by the small magnitude of the reduction in basal and agonist-induced G protein coupling using CB_2. Using 1 μM of LDK1229, in the absence of CP55,940, only reduced the basal level of [^{35}S]GTPγS binding from 95 fmol/mg to 88 fmol/mg (Figure 5B) compared to the 2-fold decrease observed with CB_1 (Figure 2A). We also observed a small decrease in the CP55,940-induced [^{35}S]GTPγS binding with an increasing concentration of LDK1229 (Figure 4B) with up to 32 μM of LDK1229 (to 110 fmol/mg from the original 120 fmol/mg). The CB_2 selective inverse agonist SR144528 (Rinaldi-Carmona et al., 1998a) antagonized the basal level of [^{35}S]GTPγS binding and is shown for comparison. We also found that LDK1229 can dock in the CB_2 inactive state model but in a higher energy conformation (data not shown). This is likely the origin of the 3-fold loss of affinity at CB_2.

Molecular Pharmacology Fast Forward. Published on November 19, 2014 as DOI: 10.1124/mol.114.095471
This article has not been copyedited and formatted. The final version may differ from this version.

DISCUSSION

In an effort to develop new modulators of the CB_1 receptor, we synthesized a group of benzhydryl piperazine analogs including the compounds LDK1203, LDK1222 and LDK1229 and describe their inverse agonist properties in this study. In addition to their inverse agonist binding profiles to the CB_1 receptor and their preference to bind the inactive T210A CB_1 receptor over the constitutively active wild-type CB_1 or fully active T210I receptor, the inverse agonism exhibited by LDK1229 was also evident from its antagonistic effect on basal and agonist-induced G protein coupling, and its ability to increase the CB_1 localization to the cell surface. LDK1229 exhibited a lower affinity for the CB_2 receptor, with relative selectivity for the CB_1 receptor of 3-fold. Because the CB_1 receptor is constitutively active both *in-vitro* and *in-vivo* (Landsman et al., 1997; Meschler et al., 2000), discovering new and improved means for inhibiting the activity of the receptor is therapeutically useful and relevant for modulating activity of the CB_1 receptor system in the brain.

Our results show that the benzhydryl piperazine analogs represented by LDK1229 behave as inverse agonists of the CB_1 receptor. Structurally, the benzhydryl piperazine analogs are distinct from the first generation of CB_1 inverse agonists, which generally possess nitrogen-containing 5- or 6-member aromatic rings as their central connecting units (Chorvat, 2013; Lange and Kruse, 2005; Vemuri et al., 2008). In contrast, benzhydryl piperazine analogs have a central core of piperazine, which is non-aromatic and possesses basic amino group(s). A pharmacophore model of the first-generation of CB_1 inverse agonists was proposed, (Lange and Kruse, 2005) of which the biaryls (e.g. SR141716A) form favorable aromatic stacking interactions with two subpockets surrounded by residues $Y5.39^{275}$-$W4.64^{255}$-$F5.42^{278}$ and residues $W5.43^{279}$-$F3.36^{200}$-$W6.48^{356}$ of CB_1. The central core (e.g. pyrazole in SR141716A)

Molecular Pharmacology Fast Forward. Published on November 19, 2014 as DOI: 10.1124/mol.114.095471
This article has not been copyedited and formatted. The final version may differ from this version.

then connects to a lipophilic moiety through a hydrogen bond acceptor (e.g. the carbonyl of SR141716A). The hydrogen bond acceptor stabilizes the D6.58^{366}-K3.28^{192} salt bridge in the inactive state of the CB_1 receptor. The lipophilic moiety (e.g. the methylene groups of piperidine ring in SR141716A) fits in a pocket formed by V3.32^{196}-F2.57^{170}-L7.43^{387} and M7.44^{384} of the CB_1 receptor (Lange and Kruse, 2005). In spite of the structural difference between our benzhydryl piperazine analogs and the first generation of CB_1 inverse agonists, docking SR141716A and LDK1229 into the CB_1 inactive state model suggest that both compounds bind in similar receptor regions and form similar interactions with the receptor. This is also consistent with the results of competitive displacement assays that suggest LDK1229 displaces SR141716A, implying an overlapping binding site. However, the results of the docking studies suggest one major difference between SR141716A and LDK1229; the geometry of the SR141716A hydrogen bond with K3.28^{192} is much better than that of LDK1229. Conformational analysis of LDK1229 suggests that it does not have the conformational freedom to adopt a conformation that would allow it to improve its hydrogen bond geometry. In addition, the extra ring hydrogen (cyclohexyl ring vs. piperidine ring) introduced in LDK1229 forces the ligand to position itself differently. Together, these effects lead to a less favorable hydrogen bond with K3.28^{192}. This is consistent with the results of the binding experiments that show that SR141716A has a higher affinity for CB_1 than does LDK1229. Notably, LDK1229 exhibits an efficacy comparable to SR141716A in antagonizing basal GTPγS binding to the CB_1 receptor although it shows a weaker binding affinity to the receptor (Table 2, Table 3 and Figure 2). One advantage of the benzhydryl piperazine analogs is that the piperazine ring provides two amino groups that can be readily used in further derivatization. This opens up rich opportunities for structural modifications that may lead to the improvement of the pharmacokinetic properties of

Molecular Pharmacology Fast Forward. Published on November 19, 2014 as DOI: 10.1124/mol.114.095471
This article has not been copyedited and formatted. The final version may differ from this version.

the drug molecules, such as their lipophilicity and polar surface area, which are critical factors influencing the brain barrier-penetration of these compounds.

Evidence has begun to emerge on the involvement of the endocannabinoid system in the regulation of metabolism in several peripheral organs crucial to energy storage and utilization (Di Marzo and Matias, 2005; Silvestri et al., 2011). Elevated peripheral endocannabinoid levels and increased CB1 expression in these tissues have been observed in several studies of obese mice (Pagotto et al., 2006) as well as obese humans compared to leaner controls (Engeli et al., 2005). In light of the above, it has proven difficult to diminish the adverse central nervous system effects of brain-penetrant CB_1 inverse agonists (Jones, 2008). Not surprisingly, significant effort has been put forth to develop CB_1 neutral antagonists (Janero, 2012) or peripherally restricted CB_1 inverse agonists (Chorvat, 2013; Silvestri and Di Marzo, 2012) that do not produce undesired central nervous system side effects. LDK1229 suggests a new lead for developing novel CB_1 inverse agonists and is attractive for the design and synthesis of peripherally active CB_1 inverse agonists, a class of potential therapeutic agents for the treatment of obesity and other related metabolic syndromes. In general, there are several strategies to reduce a ligand's permeability to the blood brain barrier (BBB) (Clark et al., 2005). These include increasing H-bonding capacity, molecular weight (MW) and polar surface area (PSA) as well as introducing acidic functional groups or increasing hydrophilicity. In comparison with the conventional scaffold of CB1 inverse agonists (i.e. biaryl substituted heteroaromatic ring), the benzhydryl piperazine scaffold offers two basic nitrogen atoms, which provide extra opportunities to increase the overall H-bonding capability. Additionally, the two basic nitrogen functionalities, are considerably easy to modify to introduce various substitutions so that the MW and PSA properties can be readily manipulated to gain suitable pharmacokinetic (PK) properties

Molecular Pharmacology Fast Forward. Published on November 19, 2014 as DOI: 10.1124/mol.114.095471
This article has not been copyedited and formatted. The final version may differ from this version.

that reduce BBB penetration. Hence, this scaffold enriches the chances for PK-driven drug optimization to achieve the desired peripheral restriction of CB1 inverse agonists.

Molecular Pharmacology Fast Forward. Published on November 19, 2014 as DOI: 10.1124/mol.114.095471
This article has not been copyedited and formatted. The final version may differ from this version.

ACKNOWLEDGMENTS

We would like to thank Sushma Samala and Hamed I. Ali for providing some technical assistance in the synthesis and chemical characterization of the benzhydryl piperazine analogs.

Molecular Pharmacology Fast Forward. Published on November 19, 2014 as DOI: 10.1124/mol.114.095471
This article has not been copyedited and formatted. The final version may differ from this version.

AUTHORSHIP CONTRIBUTIONS

Participated in research design: Mahmoud, Kendall, Lu, Olszewska, Shore, Hurst, Reggio.

Conducted experiments: Mahmoud, Olszewska, Liu, Lu, Shore.

Performed data analysis: Mahmoud, Kendall, Olszewska, Lu, Shore, Hurst, Reggio.

Wrote or contributed to the writing of the manuscript: Mahmoud, Lu, Kendall, Shore, Hurst, Reggio.

Molecular Pharmacology Fast Forward. Published on November 19, 2014 as DOI: 10.1124/mol.114.095471
This article has not been copyedited and formatted. The final version may differ from this version.

REFERENCES

Ahn KH, Bertalovitz AC, Mierke DF and Kendall DA (2009) Dual role of the second extracellular loop of the cannabinoid receptor 1: ligand binding and receptor localization. *Mol Pharmacol* **76**(4): 833-842.

Ahn KH, Mahmoud MM and Kendall DA (2012) Allosteric modulator ORG27569 induces CB1 cannabinoid receptor high affinity agonist binding state, receptor internalization, and Gi protein-independent ERK1/2 kinase activation. *J Biol Chem* **287**(15): 12070-12082.

Ballesteros JA, Jensen AD, Liapakis G, Rasmussen SG, Shi L, Gether U and Javitch JA (2001) Activation of the beta 2-adrenergic receptor involves disruption of an ionic lock between the cytoplasmic ends of transmembrane segments 3 and 6. *J Biol Chem* **276**(31): 29171-29177.

Barnett-Norris J, Hurst DP, Buehner K, Ballesteros JA, Guarnieri F and Reggio PH (2002) Agonist alkyl tail interaction with cannabinoid CB1 receptor V6.43/I6.46 groove induces a Helix 6 active conformation. *Int J Quantum Chem* **88**(1): 76-86.

Basu S and Dittel BN (2011) Unraveling the complexities of cannabinoid receptor 2 (CB2) immune regulation in health and disease. *Immunol Res* **51**(1): 26-38.

Batkai S, Jarai Z, Wagner JA, Goparaju SK, Varga K, Liu J, Wang L, Mirshahi F, Khanolkar AD, Makriyannis A, Urbaschek R, Garcia N, Jr., Sanyal AJ and Kunos G (2001) Endocannabinoids acting at vascular CB1 receptors mediate the vasodilated state in advanced liver cirrhosis. *Nat Med* **7**(7): 827-832.

Bosgraaf L, van Haastert PJ and Bretschneider T (2009) Analysis of cell movement by simultaneous quantification of local membrane displacement and fluorescent intensities using Quimp2. *Cell Motil Cytoskeleton* **66**(3): 156-165.

Bouaboula M, Poinot-Chazel C, Marchand J, Canat X, Bourrie B, Rinaldi-Carmona M, Calandra B, Le Fur G and Casellas P (1996) Signaling pathway associated with stimulation of CB2 peripheral cannabinoid receptor. Involvement of both mitogen-activated protein kinase and induction of Krox-24 expression. *Eur J Biochem* **237**(3): 704-711.

Chen C and Okayama H (1987) High-efficiency transformation of mammalian cells by plasmid DNA. *Mol Cell Biol* **7**(8): 2745-2752.

Cheng Y and Prusoff WH (1973) Relationship between the inhibition constant (K1) and the concentration of inhibitor which causes 50 per cent inhibition (I50) of an enzymatic reaction. *Biochem Pharmacol* **22**(23): 3099-3108.

Chorvat RJ (2013) Peripherally restricted CB1 receptor blockers. *Bioorg Med Chem Lett* **23**(17): 4751-4760.

Clark DE, Doherty A, Bock M, Desai M, Overington J, Plattner J, Stamford A, Wustrow D and Young H (2005) Computational prediction of blood-brain barrier permeation. *Annu Rep Med Chem* **40**: 403.

Cotecchia S, Exum S, Caron MG and Lefkowitz RJ (1990) Regions of the alpha 1-adrenergic receptor involved in coupling to phosphatidylinositol hydrolysis and enhanced sensitivity of biological function. *Proc Natl Acad Sci U S A* **87**(8): 2896-2900.

Croci T, Manara L, Aureggi G, Guagnini F, Rinaldi-Carmona M, Maffrand JP, Le Fur G, Mukenge S and Ferla G (1998) In vitro functional evidence of neuronal cannabinoid CB1 receptors in human ileum. *Br J Pharmacol* **125**(7): 1393-1395.

D'Antona AM, Ahn KH and Kendall DA (2006) Mutations of CB1 T210 produce active and inactive receptor forms: correlations with ligand affinity, receptor stability, and cellular localization. *Biochemistry* **45**(17): 5606-5617.

De Lean A, Stadel JM and Lefkowitz RJ (1980) A ternary complex model explains the agonist-specific binding properties of the adenylate cyclase-coupled beta-adrenergic receptor. *J Biol Chem* **255**(15): 7108-7117.

Despres JP, Golay A, Sjostrom L and Rimonabant in Obesity-Lipids Study G (2005) Effects of rimonabant on metabolic risk factors in overweight patients with dyslipidemia. *N Engl J Med* **353**(20): 2121-2134.

Di Marzo V and Matias I (2005) Endocannabinoid control of food intake and energy balance. *Nat Neurosci* **8**(5): 585-589.

Dormann D, Libotte T, Weijer CJ and Bretschneider T (2002) Simultaneous quantification of cell motility and protein-membrane-association using active contours. *Cell Motil Cytoskeleton* **52**(4): 221-230.

Engeli S, Bohnke J, Feldpausch M, Gorzelniak K, Janke J, Batkai S, Pacher P, Harvey-White J, Luft FC, Sharma AM and Jordan J (2005) Activation of the peripheral endocannabinoid system in human obesity. *Diabetes* **54**(10): 2838-2843.

Fay JF, Dunham TD and Farrens DL (2005) Cysteine residues in the human cannabinoid receptor: only C257 and C264 are required for a functional receptor, and steric bulk at C386 impairs antagonist SR141716A binding. *Biochemistry* **44**(24): 8757-8769.

Galiegue S, Mary S, Marchand J, Dussossoy D, Carriere D, Carayon P, Bouaboula M, Shire D, Le Fur G and Casellas P (1995) Expression of central and peripheral cannabinoid receptors in human immune tissues and leukocyte subpopulations. *Eur J Biochem* **232**(1): 54-61.

Gerard CM, Mollereau C, Vassart G and Parmentier M (1991) Molecular cloning of a human cannabinoid receptor which is also expressed in testis. *Biochem J* **279 (Pt 1)**: 129-134.

Gether U and Kobilka BK (1998) G protein-coupled receptors. II. Mechanism of agonist activation. *J Biol Chem* **273**(29): 17979-17982.

Ghanouni P, Steenhuis JJ, Farrens DL and Kobilka BK (2001) Agonist-induced conformational changes in the G-protein-coupling domain of the beta 2 adrenergic receptor. *Proc Natl Acad Sci U S A* **98**(11): 5997-6002.

Hildebrand PW, Scheerer P, Park JH, Choe HW, Piechnick R, Ernst OP, Hofmann KP and Heck M (2009) A ligand channel through the G protein coupled receptor opsin. *PLoS ONE* **4**(2): e4382.

Howlett AC (1995) Pharmacology of cannabinoid receptors. *Annu Rev Pharmacol Toxicol* **35**: 607-634.

Howlett AC (2005) Cannabinoid receptor signaling. *Handb Exp Pharmacol* (168): 53-79.

Howlett AC, Breivogel CS, Childers SR, Deadwyler SA, Hampson RE and Porrino LJ (2004) Cannabinoid physiology and pharmacology: 30 years of progress. *Neuropharmacology* **47 Suppl 1**: 345-358.

Howlett AC and Fleming RM (1984) Cannabinoid inhibition of adenylate cyclase. Pharmacology of the response in neuroblastoma cell membranes. *Mol Pharmacol* **26**(3): 532-538.

Hurst D, Umejiego U, Lynch D, Seltzman H, Hyatt S, Roche M, McAllister S, Fleischer D, Kapur A, Abood M, Shi S, Jones J, Lewis D and Reggio P (2006) Biarylpyrazole inverse agonists at the cannabinoid CB1 receptor: importance of the C-3 carboxamide oxygen/lysine3.28(192) interaction. *J Med Chem* **49**(20): 5969-5987.

Hurst DP, Grossfield A, Lynch DL, Feller S, Romo TD, Gawrisch K, Pitman MC and Reggio PH (2010) A lipid pathway for ligand binding is necessary for a cannabinoid G protein-coupled receptor. *J Biol Chem* **285**(23): 17954-17964.

Hurst DP, Lynch DL, Barnett-Norris J, Hyatt SM, Seltzman HH, Zhong M, Song ZH, Nie J, Lewis D and Reggio PH (2002) N-(piperidin-1-yl)-5-(4-chlorophenyl)-1-(2,4-dichlorophenyl)-4-methyl-1H-p yrazole-3-carboxamide (SR141716A) interaction with LYS 3.28(192) is crucial for its inverse agonism at the cannabinoid CB1 receptor. *Mol Pharmacol* **62**(6): 1274-1287.

Janero DR (2012) Cannabinoid-1 receptor (CB1R) blockers as medicines: beyond obesity and cardiometabolic disorders to substance abuse/drug addiction with CB1R neutral antagonists. *Expert Opin Emerg Drugs* **17**(1): 17-29.

Janero DR and Makriyannis A (2009) Cannabinoid receptor antagonists: pharmacological opportunities, clinical experience, and translational prognosis. *Expert Opin Emerg Drugs* **14**(1): 43-65.

Jones D (2008) End of the line for cannabinoid receptor 1 as an anti-obesity target? *Nature Reviews Drug Discovery* **7**(12): 961-962.

Kenakin T (1995) Agonist-receptor efficacy. II. Agonist trafficking of receptor signals. *Trends Pharmacol Sci* **16**(7): 232-238.

Landsman RS, Burkey TH, Consroe P, Roeske WR and Yamamura HI (1997) SR141716A is an inverse agonist at the human cannabinoid CB1 receptor. *Eur J Pharmacol* **334**(1): R1-2.

Lange JH and Kruse CG (2005) Keynote review: Medicinal chemistry strategies to CB1 cannabinoid receptor antagonists. *Drug Discov Today* **10**(10): 693-702.

Lange JH and Kruse CG (2008) Cannabinoid CB1 receptor antagonists in therapeutic and structural perspectives. *Chem Rec* **8**(3): 156-168.

Leterrier C, Bonnard D, Carrel D, Rossier J and Lenkei Z (2004) Constitutive endocytic cycle of the CB1 cannabinoid receptor. *J Biol Chem* **279**(34): 36013-36021.

Mackie K (2006) Cannabinoid receptors as therapeutic targets. *Annu Rev Pharmacol Toxicol* **46**: 101-122.

Marcu J, Shore DM, Kapur A, Trznadel M, Makriyannis A, Reggio PH and Abood ME (2013) Novel insights into CB1 cannabinoid receptor signaling: a key interaction identified between the extracellular-3 loop and transmembrane helix 2. *J Pharmacol Exp Ther* **345**(2): 189-197.

Marion S, Weiner DM and Caron MG (2004) RNA editing induces variation in desensitization and trafficking of 5-hydroxytryptamine 2c receptor isoforms. *J Biol Chem* **279**(4): 2945-2954.

Martini L, Waldhoer M, Pusch M, Kharazia V, Fong J, Lee JH, Freissmuth C and Whistler JL (2007) Ligand-induced down-regulation of the cannabinoid 1 receptor is mediated by the G-protein-coupled receptor-associated sorting protein GASP1. *FASEB J* **21**(3): 802-811.

McAllister SD, Hurst DP, Barnett-Norris J, Lynch D, Reggio PH and Abood ME (2004) Structural mimicry in class A G protein-coupled receptor rotamer toggle switches: the importance of the F3.36(201)/W6.48(357) interaction in cannabinoid CB1 receptor activation. *J Biol Chem* **279**(46): 48024-48037.

McAllister SD, Rizvi G, Anavi-Goffer S, Hurst DP, Barnett-Norris J, Lynch DL, Reggio PH and Abood ME (2003) An aromatic microdomain at the cannabinoid CB(1) receptor constitutes an agonist/inverse agonist binding region. *J Med Chem* **46**(24): 5139-5152.

McWhinney C, Wenham D, Kanwal S, Kalman V, Hansen C and Robishaw JD (2000) Constitutively active mutants of the alpha(1a)- and the alpha(1b)-adrenergic receptor subtypes reveal coupling to different signaling pathways and physiological responses in rat cardiac myocytes. *J Biol Chem* **275**(3): 2087-2097.

Meschler JP, Kraichely DM, Wilken GH and Howlett AC (2000) Inverse agonist properties of N-(piperidin-1-yl)-5-(4-chlorophenyl)-1-(2, 4-dichlorophenyl)-4-methyl-1H-pyrazole-3-carboxamide HCl (SR141716A) and 1-(2-chlorophenyl)-4-cyano-5-(4-methoxyphenyl)-1H-pyrazole-3-carboxyl ic acid phenylamide (CP-272871) for the CB(1) cannabinoid receptor. *Biochem Pharmacol* **60**(9): 1315-1323.

Moreira FA and Crippa JA (2009) The psychiatric side-effects of rimonabant. *Rev Bras Psiquiatr* **31**(2): 145-153.

Muccioli G and Lambert D (2005) Current knowledge on the antagonists and inverse agonists of cannabinoid receptors. *Curr Med Chem* **12**(12): 1361-1394.

Pagotto U, Marsicano G, Cota D, Lutz B and Pasquali R (2006) The emerging role of the endocannabinoid system in endocrine regulation and energy balance. *Endocr Rev* **27**(1): 73-100.

Palczewski K, Kumasaka T, Hori T, Behnke CA, Motoshima H, Fox BA, Le Trong I, Teller DC, Okada T, Stenkamp RE, Yamamoto M and Miyano M (2000) Crystal structure of rhodopsin: A G protein-coupled receptor. *Science* **289**(5480): 739-745.

Park JH, Scheerer P, Hofmann KP, Choe HW and Ernst OP (2008) Crystal structure of the ligand-free G-protein-coupled receptor opsin. *Nature* **454**(7201): 183-187.

Pei Y, Mercier RW, Anday JK, Thakur GA, Zvonok AM, Hurst D, Reggio PH, Janero DR and Makriyannis A (2008) Ligand-binding architecture of human CB2 cannabinoid receptor: evidence for receptor subtype-specific binding motif and modeling GPCR activation. *Chem Biol* **15**(11): 1207-1219.

Pertwee RG (2005) Inverse agonism and neutral antagonism at cannabinoid CB1 receptors. *Life Sci* **76**(12): 1307-1324.

Pertwee RG (2006) Cannabinoid pharmacology: the first 66 years. *Br J Pharmacol* **147 Suppl 1**: S163-171.

Picone RP, Khanolkar AD, Xu W, Ayotte LA, Thakur GA, Hurst DP, Abood ME, Reggio PH, Fournier DJ and Makriyannis A (2005) (-)-7'-Isothiocyanato-11-hydroxy-1',1'-dimethylheptylhexahydrocannabinol (AM841), a high-affinity electrophilic ligand, interacts covalently with a cysteine in helix six and activates the CB1 cannabinoid receptor. *Mol Pharmacol* **68**(6): 1623-1635.

Rinaldi-Carmona M, Barth F, Heaulme M, Shire D, Calandra B, Congy C, Martinez S, Maruani J, Neliat G, Caput D and et al. (1994) SR141716A, a potent and selective antagonist of the brain cannabinoid receptor. *FEBS Lett* **350**(2-3): 240-244.

Rinaldi-Carmona M, Barth F, Millan J, Derocq JM, Casellas P, Congy C, Oustric D, Sarran M, Bouaboula M, Calandra B, Portier M, Shire D, Breliere JC and Le Fur GL (1998a) SR 144528, the first potent and selective antagonist of the CB2 cannabinoid receptor. *J Pharmacol Exp Ther* **284**(2): 644-650.

Rinaldi-Carmona M, Le Duigou A, Oustric D, Barth F, Bouaboula M, Carayon P, Casellas P and Le Fur G (1998b) Modulation of CB1 cannabinoid receptor functions after a long-term exposure to agonist or inverse agonist in the Chinese hamster ovary cell expression system. *J Pharmacol Exp Ther* **287**(3): 1038-1047.

Rozenfeld R and Devi LA (2008) Regulation of CB1 cannabinoid receptor trafficking by the adaptor protein AP-3. *FASEB J* **22**(7): 2311-2322.

Scheerer P, Park JH, Hildebrand PW, Kim YJ, Krauss N, Choe HW, Hofmann KP and Ernst OP (2008) Crystal structure of opsin in its G-protein-interacting conformation. *Nature* **455**(7212): 497-502.

Shim JY, Bertalovitz AC and Kendall DA (2012) Probing the interaction of SR141716A with the CB1 receptor. *J Biol Chem* **287**(46): 38741-38754.

Silvestri C and Di Marzo V (2012) Second generation CB1 receptor blockers and other inhibitors of peripheral endocannabinoid overactivity and the rationale of their use against metabolic disorders. *Expert Opin Investig Drugs* **21**(9): 1309-1322.

Silvestri C, Ligresti A and Di Marzo V (2011) Peripheral effects of the endocannabinoid system in energy homeostasis: adipose tissue, liver and skeletal muscle. *Rev Endocr Metab Disord* **12**(3): 153-162.

Slipetz DM, O'Neill GP, Favreau L, Dufresne C, Gallant M, Gareau Y, Guay D, Labelle M and Metters KM (1995) Activation of the human peripheral cannabinoid receptor results in inhibition of adenylyl cyclase. *Mol Pharmacol* **48**(2): 352-361.

Song ZH and Bonner TI (1996) A lysine residue of the cannabinoid receptor is critical for receptor recognition by several agonists but not WIN55212-2. *Mol Pharmacol* **49**(5): 891-896.

Traynor K (2007) Panel advises against rimonabant approval. *Am J Health Syst Pharm* **64**(14): 1460-1461.

Turu G and Hunyady L (2010) Signal transduction of the CB1 cannabinoid receptor. *J Mol Endocrinol* **44**(2): 75-85.

Vemuri VK, Janero DR and Makriyannis A (2008) Pharmacotherapeutic targeting of the endocannabinoid signaling system: drugs for obesity and the metabolic syndrome. *Physiol Behav* **93**(4-5): 671-686.

Visiers I, Ebersole BJ, Dracheva S, Ballesteros J, Sealfon SC and Weinstein H (2002) Structural motifs as functional microdomains in G-protein-coupled receptors: Energetic

considerations in the mechanism of activation of the serotonin 5-HT2a receptor by disruption of the ionic lock of the arginine cage. *Int J Quantum Chem* **88**: 65-75.

Wade SM, Lan K, Moore DJ and Neubig RR (2001) Inverse agonist activity at the alpha(2A)-adrenergic receptor. *Mol Pharmacol* **59**(3): 532-542.

Weïwer M, Bittker JA, Lewis TA, Shimada K, Yang WS, MacPherson L, Dandapani S, Palmer M, Stockwell BR and Schreiber SL (2012) Development of small-molecule probes that selectively kill cells induced to express mutant RAS. *Bioorg Med Chem Lett* **22**(4): 1822-1826.

Molecular Pharmacology Fast Forward. Published on November 19, 2014 as DOI: 10.1124/mol.114.095471
This article has not been copyedited and formatted. The final version may differ from this version.

FOOTNOTES

Sources of financial support:

This work was supported in part by National Institutes of Health [Grant DA020763], [Grants DA003934 and DA021358], and by the Faculty Development Fund of Texas A&M Health Sciences Center.

Reprint requests to be sent to:

Debra A. Kendall
Department of Pharmaceutical Sciences, University of Connecticut, 06269
Phone: (860) 486-1891; Fax: (860) 486-2693
Email: debra.kendall@uconn.edu.

Conflict of interest:

The authors declare no conflict of interest.

Molecular Pharmacology Fast Forward. Published on November 19, 2014 as DOI: 10.1124/mol.114.095471
This article has not been copyedited and formatted. The final version may differ from this version.

Figure Legends

Figure 1. Compound structures. (A) Synthesis of benzhydryl piperazine analogs LDK1203, LDK1222 and LDK1229. a) Oxalyl chloride, DCM, cat. DMF; b) Piperazine, CH_3CN; c) 3-Bromo-1-phenyl-1-propene, K_2CO_3, DMF; d) TsCl, DIPEA, DCM; e) Cyclohexanecarbonyl chloride, DIPEA, DCM; f) 1.0 M HCl in ether. **(B)** Representative members of the first generation of CB_1 inverse agonists are shown for comparison.

Figure 2. Effect of LDK1229 and LDK1203 on the stimulation of [^{35}S] GTPγS binding to HEK293 cell membranes expressing the CB_1 wild-type receptor. (A) The basal level of [^{35}S] GTPγS binding was measured for the CB_1 wild-type receptor. The stimulatory effect of CP55,940 and the inhibitory effects of SR141716A, LDK1229 and LDK1203 on [^{35}S] GTPγS binding were measured at the indicated concentrations. Statistical significance of the differences compared to basal was assessed using one-way analysis of variance and Bonferroni's post hoc test: $*p < 0.05$, $**p < 0.01$, and $***p < 0.001$. **(B)** The inhibitory effects of both LDK1229 and LDK1203 on CP55,940-induced [^{35}S] GTPγS binding in membrane preparations. Statistical significance of the differences compared to 0.1μM CP55,940 alone was assessed using one-way analysis of variance and Bonferroni's post hoc test: $\dagger p < 0.05$, $\dagger\dagger p < 0.01$, and $\dagger\dagger\dagger p < 0.001$. Data are presented as specific binding of GTPγS to the membranes. Nonspecific binding was determined in the presence of 10 μM unlabeled GTPγS. Each data point represents the mean ± S.E. (*error bars*) of at least 3 independent experiments performed in duplicate. The *dotted line* indicates the level of non CB_1-mediated GTPγS binding obtained from GTPγS binding to the mock-transfected membrane sample.

Molecular Pharmacology Fast Forward. Published on November 19, 2014 as DOI: 10.1124/mol.114.095471
This article has not been copyedited and formatted. The final version may differ from this version.

Figure 3. The effect of LDK1229 on internalization of the CB_1 receptor. (A) HEK293 cells expressing the CB_1-GFP receptor were incubated with vehicle alone (0.03% DMSO), 0.5 μM SR141716A or 10 μM LDK1229. SR141716A is shown for comparison. **(B)** Quantification of CB_1 receptors on the cell surface. The QuimP software with plug-ins was used as described in Materials and Methods. Images are representative of at least four independent transfections. The scale bar is 5μm.

Figure 4. Model of LDK1229 docked in the inactive CB_1 receptor model. (A) and **(C)** illustrate SR141716A (shown in cyan) docked in the CB_1 inactive state model. **(B)** and **(D)** illustrate the final docked conformation of LDK1229 (shown in lavender) in the CB_1 inactive state model. Hydrogen bonds are shown in yellow, aromatic microdomain residues are shown in orange, and hydrophobic interactions are shown in lime.

Figure 5. The binding parameters of LDK1229 and LDK1203 to CB_2. (A) Binding of LDK1229 and LDK1203 to CB_2 wild-type receptors and **(B)** their effect on the stimulation of [^{35}S] GTPγS binding. Statistical significance of the differences (*compared to basal, †compared to 0.1μM CP55,940 alone) was assessed using one-way analysis of variance and Bonferroni's post hoc test: *$p < 0.05$, **$p < 0.01$, and ***$p < 0.001$; †$p < 0.05$, ††$p < 0.01$, and †††$p < 0.001$.

PDB. A homology model illustrating the final docked conformation of LDK1229 in the CB_1 inactive state model.

Table 1. LDK1203 and LDK1222 binding to the wild-type CB_1 receptor.

	vs. [^{3}H]CP55,940			vs. [^{3}H] SR141716A		
	K_i (nM)[a]			K_i (nM)		
	CP55,940	LDK1203	LDK1222	SR141716A	LDK1203	LDK1222
CB1 wild-type	2.56 (1.45-4.51)[b]	260 (80.7-837)	331 (177-619)	5.23 (3.29-8.32)[b]	297 (192-458)	366 (144-928)

[a]Data are the median and corresponding 95% confidence limits of three independent experiments performed in duplicate. K_i values were determined from competition binding assays using [^{3}H]CP55,940 or [^{3}H]SR141716A as tracers at their respective K_d values as described in Results.

[b]Binding values are from Ahn et.al., 2009 for comparison.

Molecular Pharmacology Fast Forward. Published on November 19, 2014 as DOI: 10.1124/mol.114.095471
This article has not been copyedited and formatted. The final version may differ from this version.

Table 2. LDK1229 binding to the T210A, wild-type and T210I CB_1 receptors using [^{3}H]SR141716A as a tracer.

	K_i (nM)[a]			
	SR141716A	K_i ratio (wild-type : mutant)	LDK1229	K_i ratio (wild-type : mutant)
CB1 T210A	1.47 (1.14-1.90)	4:1	67.4 (34.7-131)	3:1
CB1 wild-type	5.23 (3.29-8.32)[b]	1:1	246 (164-367)	1:1
CB1 T210I	14.7 (9.61-23.1)	1:3	NB[c]	-

[a]Data are the median and corresponding 95% confidence limits of three independent experiments performed in duplicate. K_i values were determined from competition binding assays using [^{3}H]SR141716A as tracers at its respective K_d values as described in Results.

[b]Binding values are from Ahn et al. 2009 for comparison.

[c]NB: no binding using up to 32 μM of LDK compound.

Molecular Pharmacology Fast Forward. Published on November 19, 2014 as DOI: 10.1124/mol.114.095471
This article has not been copyedited and formatted. The final version may differ from this version.

Table 3. LDK1229 binding to the T210A, wild-type and T210I CB_1 receptors using [^{3}H]CP55,940 as a tracer.

	K_i (nM)[a]			
	CP55,940	K_i ratio (wild-type : mutant)	LDK1229	K_i ratio (wild-type : mutant)
CB1 T210A	7.00 (2.59-18.9)	1:3	NB[c]	-
CB1 wild-type	2.56 (1.45-4.51)[b]	1:1	220 (106-457)	1:1
CB1 T210I	0.835 (0.542-1.29)	3:1	5831 (907-7510)	1:27

[a]Data are the median and corresponding 95% confidence limits of three independent experiments performed in duplicate. K_i values were determined from competition binding assays using [^{3}H]CP55,940 as tracer at its respective K_d values as described in Results.

[b]Binding values are from Ahn et al. 2009 for comparison.

[c]NB: no binding using up to 32 μM of LDK compound.

Molecular Pharmacology Fast Forward. Published on November 19, 2014 as DOI: 10.1124/mol.114.095471
This article has not been copyedited and formatted. The final version may differ from this version.

Table 4. LDK1229 binding to the wild-type or mutant CB_1 receptors using [^{3}H]CP55,940 or [^{3}H]WIN55,212-2 as a tracer.

	K_i [a]	
	[^{3}H]CP55,940	
Receptor	nM	K_i ratio (wild-type : mutant)
CB1 wild-type	220 (106-457)	1:1
K3.28^{192}A	1316 (1115-1626)[b]	1:4[b]
W5.43^{279}A	ND[c]	-
W6.48^{356}A	1987 (895-2736)	1:9
C7.42^{386}M	1010 (832-1154)	1:5

[a]Data are the median and corresponding 95% confidence limits of three independent experiments performed in duplicate. K_i values were determined from competition binding assays using [^{3}H]CP55,940 as tracer at its respective K_d values as described in Results.

[b]Binding was performed with [^{3}H]WIN55,212-2 as a tracer. LDK1229 binding to CB1 wild-type using [^{3}H]WIN55,212-2 as a tracer yielded a Ki= 324 nM (205-524).

[c]ND: not detectable; 39% displacement at 32 μM.

Figure 1

A

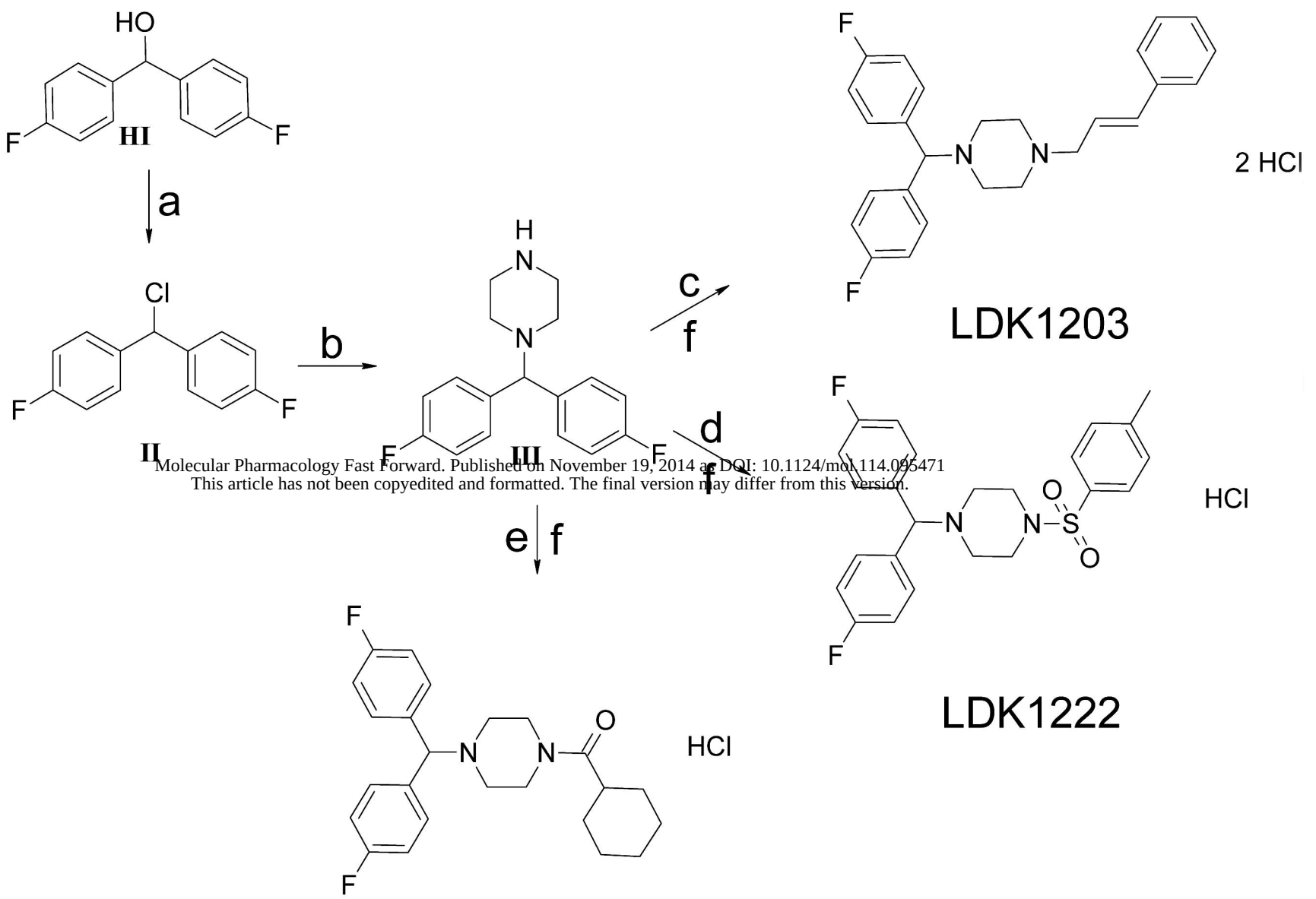

B

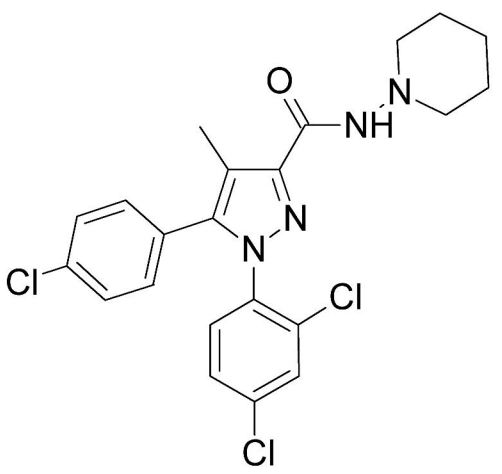

Rimonabant
(SR141716A)

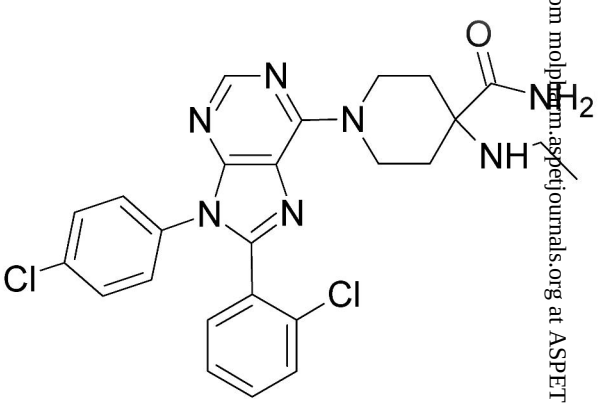

Otenabant
(CP-945,598)

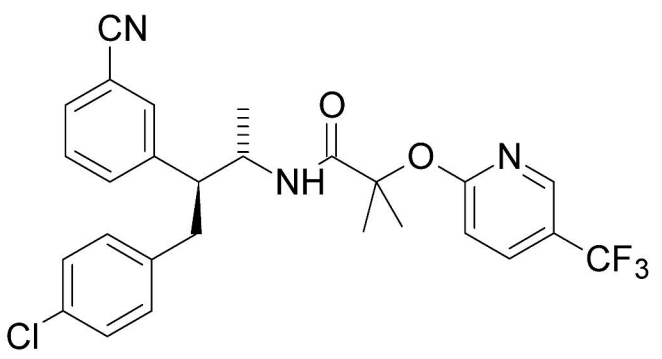

Taranabant
(MK-0364)

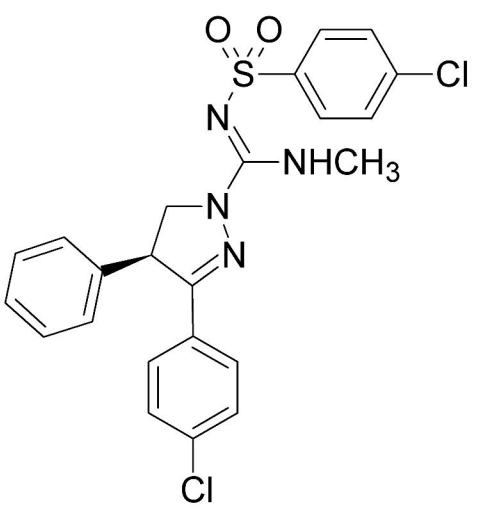

Ibipinabant
(SLV-319)

Figure 2

A

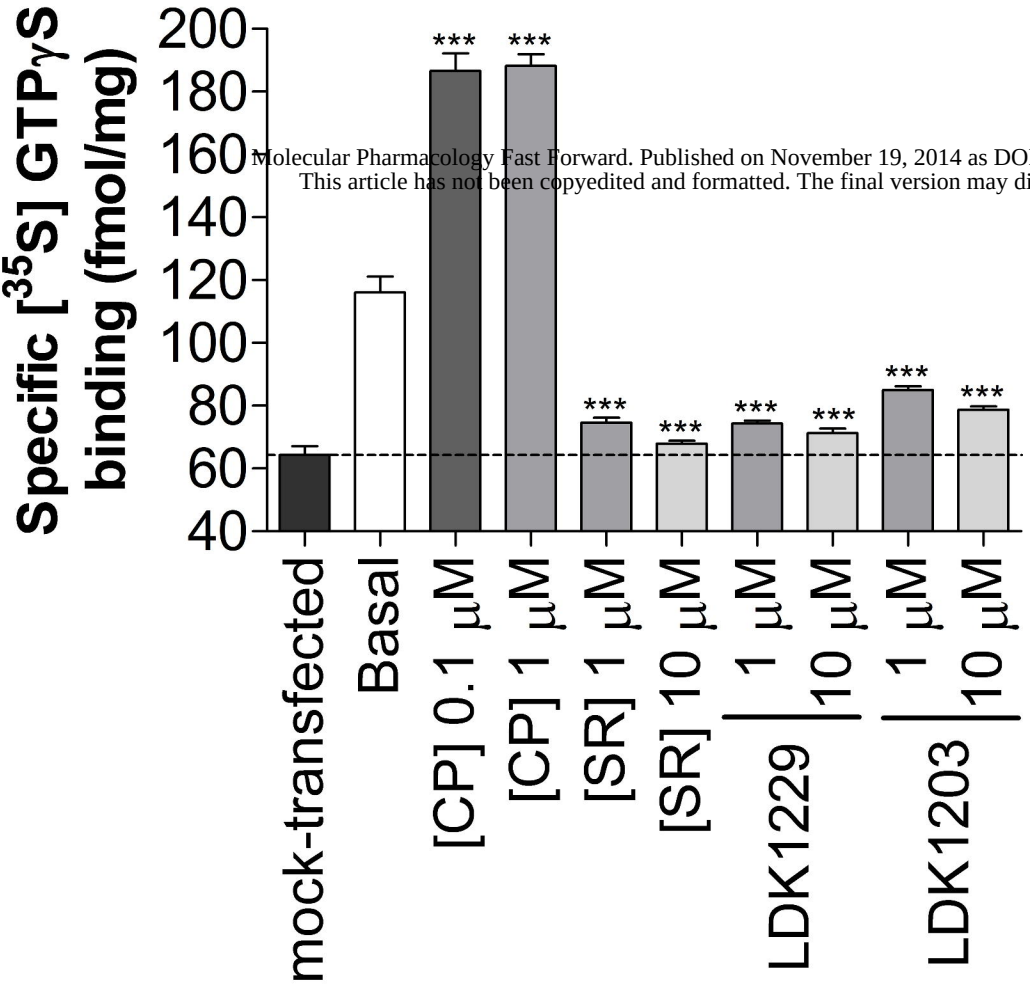

B

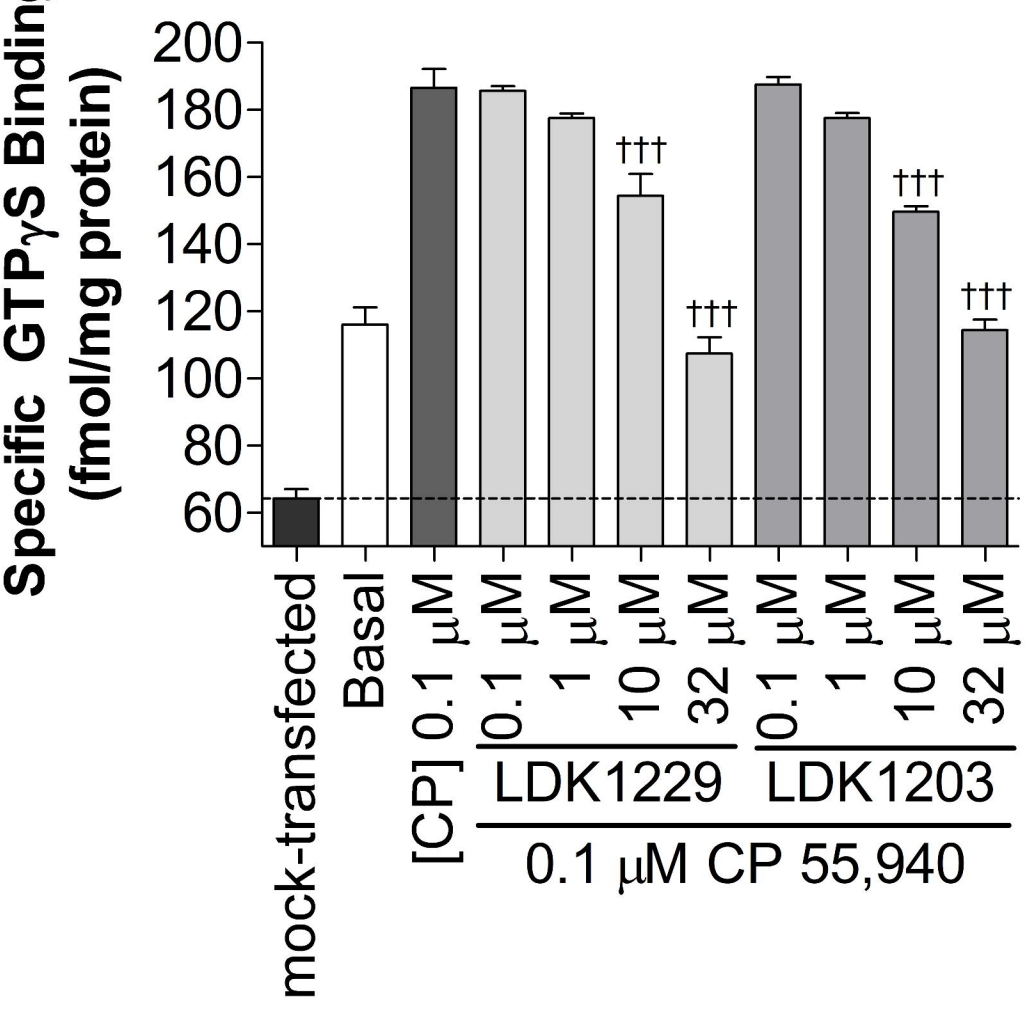

Figure 3

A

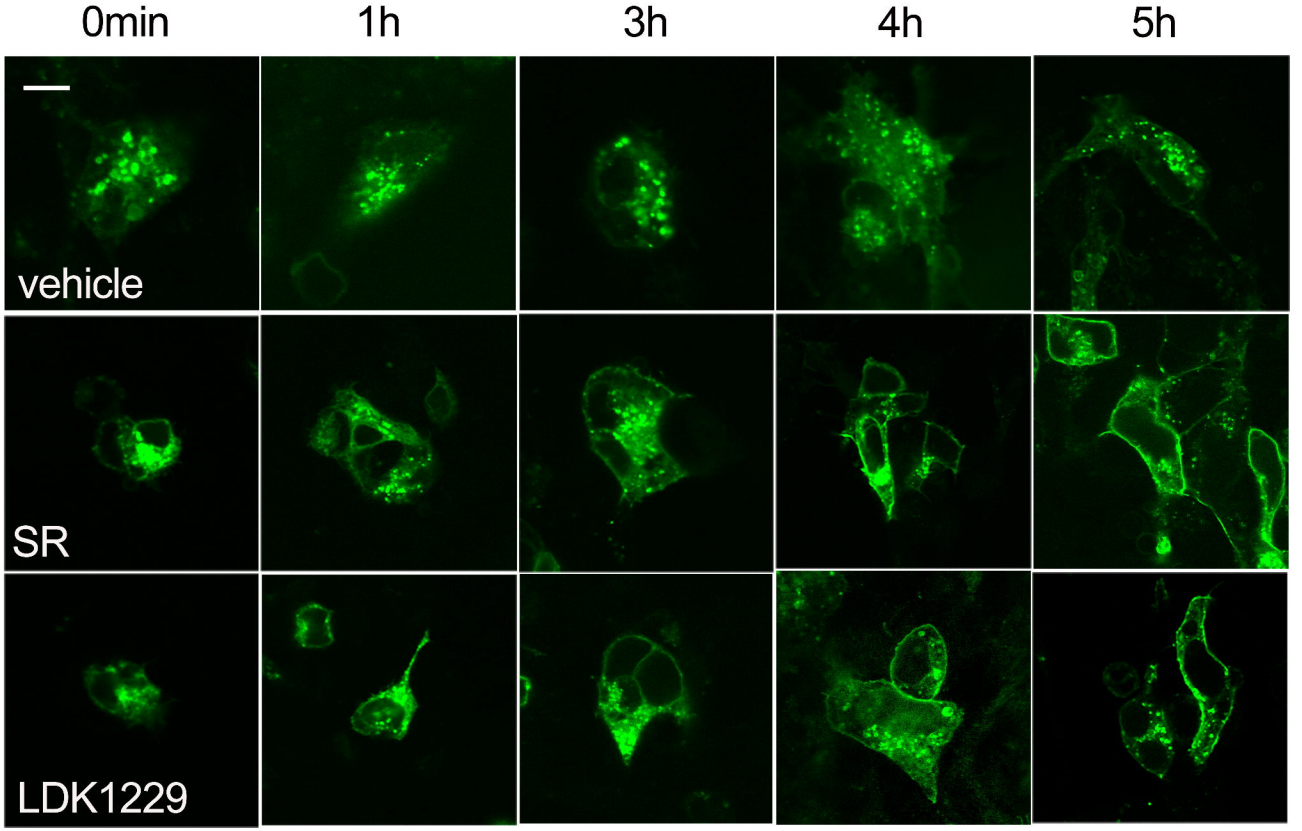
0min
1h
3h
4h
5h
vehicle
SR
LDK1229

B

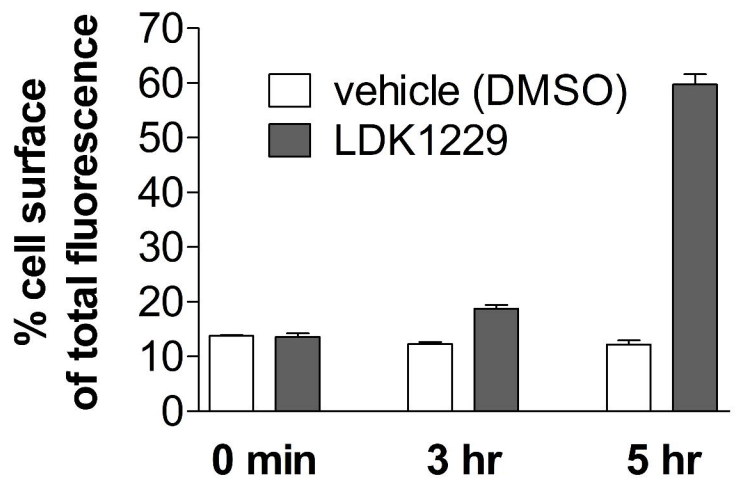
% cell surface of total fluorescence
70
60
50
40
30
20
10
0
vehicle (DMSO)
LDK1229
0 min
3 hr
5 hr

Figure 4

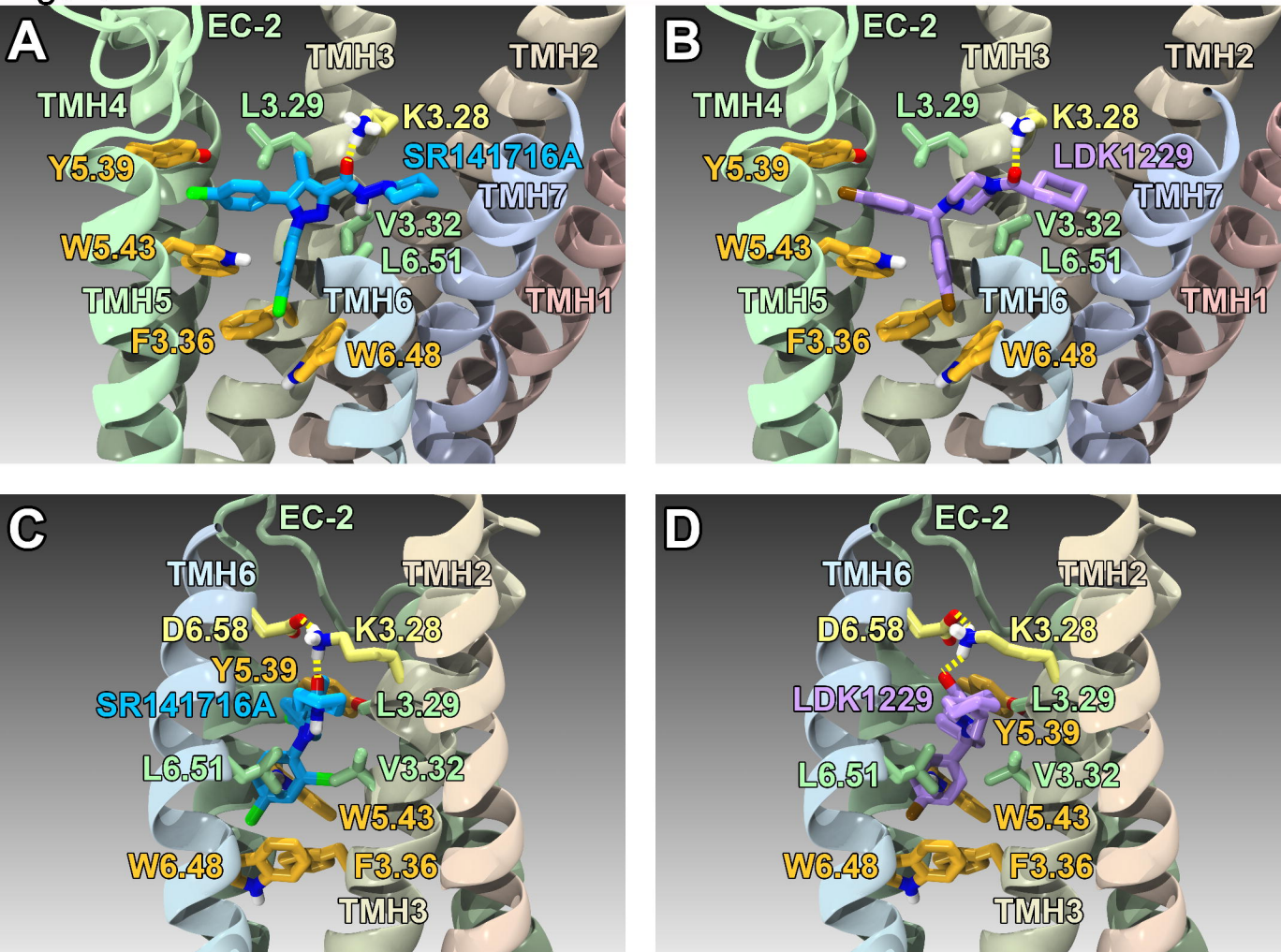
A
EC-2
TMH3
TMH2
TMH4
L3.29
K3.28
SR141716A
Y5.39
TMH7
V3.32
W5.43
L6.51
TMH5
TMH6
TMH1
F3.36
W6.48
B
EC-2
TMH3
TMH2
TMH4
L3.29
K3.28
LDK1229
Y5.39
TMH7
V3.32
W5.43
L6.51
TMH5
TMH6
TMH1
F3.36
W6.48
C
EC-2
TMH6
TMH2
D6.58
K3.28
Y5.39
SR141716A
L3.29
L6.51
V3.32
W5.43
W6.48
F3.36
TMH3
D
EC-2
TMH6
TMH2
D6.58
K3.28
LDK1229
L3.29
Y5.39
L6.51
V3.32
W5.43
W6.48
F3.36
TMH3

Figure 5

A

	[^{3}H] CP55,940		
	K_i (nM)		
	CP55,940	LDK1229	LDK1203
CB2 WT	1.7 (1.0-2.9)	632.9 (282.4-1418)	NB [a]

[a] NB: no detectable binding using up to 32 μM of LDK compound

B